The 11th Cool Stars, Stellar Systems and the Sun
ASP Conference Series, Vol. 223, 2001
R. J. García López, R. Rebolo, M. R. Zapatero Osorio, eds.

Spatially Resolved Tomographic STIS Spectroscopy of Betelgeuse[3]

A. Lobel[1], A. K. Dupree[1], and R. L. Gilliland[2]

Abstract. We present a spectral analysis of the cool supergiant α Ori (M2 Iab) based on near-UV, optical and near-IR spectra obtained between Feb. '93 and March '99 with the Space Telescope Imaging Spectrograph (STIS), the Utrecht Echelle Spectrograph (UES-WHT) and the high-resolution SOFIN spectrograph (Nordic Optical Telescope). The STIS spectra are spatially resolved by scanning across the UV disk of the star. They reveal complex dynamical velocity fields across the stellar chromosphere, which confirm subtle and variable intensity patterns monitored simultaneously in the UV with the Faint Object Camera.

A detailed spectral non-LTE modeling of the Mg II h & k and Si I resonance emission line profiles permits us to determine small changes in the chromospheric velocity structure, combined with kinetic temperature and density variations derived from radiative transfer fits to the Hα absorption line, by accounting for effects of spherical geometry in this extended atmosphere. We observe that intensity changes of the latter line core are correlated in time with weaker intensity changes seen in prominent TiO band-heads, which dominate the optical spectrum. Detailed line fits to unblended photospheric metal absorption lines, observed in July '99 with high resolution near 1 μm, yield $T_{\rm eff}$=3500$\pm$100 K and $\log(g)$=$-$0.5 with solar metallicity and 12$\pm$1 km s^{-1} for macrobroadening and $V \sin i$. However our best fits to molecular bands in the optical also hint of temperature effects of the chromosphere on the observed molecular band-strengths.

We present a semi-empirically constrained model of the chromosphere of *Betelgeuse* with a maximum kinetic temperature of 5400 K, showing variations which do not exceed $\sim$400 K over time. The model fits require highly supersonic microturbulent velocities ranging up to 19 km s^{-1}, in strong contrast with the photospheric value of only 2$\pm$1 km s^{-1}. A detailed profile study of strong UV emission lines of Si I, Mg II and Fe II reveal small Doppler shifts of 4 to 8 km s^{-1} in these self-absorbed cores (observed with STIS between Jan. '98 and March '99), which we model by changes in the outer chromospheric velocity field. These Doppler shifts correlate with the strong intensity variations

[1]Smithsonian Astrophysical Observatory, 60 Garden Street, Cambridge, MA 02138 USA

[2]Space Telescope Science Institute, 3700 San Martin Drive, Baltimore, MD 21218 USA

[3]Based on observations with the NASA/ESA *Hubble Space Telescope*, obtained at the Space Telescope Science Institute which is operated by AURA Inc. under NASA contract NAS5-26555

observed in the longwave emission component of these lines. When compared to the STIS spectra these fluxes appeared particularly intense in Sept. '92, observed with the Goddard High Resolution Spectrograph, indicating a phase of enhanced chromospheric outflow in 1992.

1. Observations

STIS spectra of *Betelgeuse* were obtained on Jan. 8, April 1, Sept. 21 '98 and on March 28 '99 with medium dispersion (R∼30,000) between 2300 Å and 3100 Å. The field of view on the UV stellar disk (∼120 mas) was confined using a slit-width of 25 mas by 100 mas. An intensity peak-up in this aperture determines the central target position 0.0 on the stellar disk (Fig. 1). The disk is then tomographically scanned in opposite directions in three off-sets of 25 mas, providing spatially resolved echelle spectra. One observation on April 1 '98 with the E230H high-resolution grating provided spectra with R=114,000 at 5 dithering positions in off-sets of 63 mas, but for a larger slit-width of 63 mas by 200 mas. The spectra have been re-calibrated by us using the *calstis* software under STSDAS IRAF, utilizing the updated STIS aperture throughput tables.

The FOC image of *Betelgeuse* shown in Fig. 1 was derived on Sept. 14 '98, about a week before the STIS spectra. This image is a sum image of four separate exposures in a passband centered at 2530 Å, taken under different pointing off-sets of about half a pixel size (1 pixel width is 14.3 mas). This dithering procedure increases the spatial resolution of the sum image after co-aligning the exposures. Note the brighter 'comma-like' pattern seen across the disk. The STIS spectral scan which corresponds to this image shows a symmetric weakening of prominent emission lines when scanning toward the limb. This intensity distribution appeared however asymmetric on April 1 '98, which results from a more 'spot-like' brightness pattern seen in the eastern disk quadrant (for a discussion see Dupree et al. 1999). We also observe that the short- and long-wavelength flux levels of many self-absorbed near-UV emission lines display variable intensity ratios when scanning across the disk, which we attribute to small differences in the mean atmospheric/chromospheric velocity fields of the scattering material in the line of sight for every aperture position.

2. Photospheric model parameters

Two optical echelle spectra of *Betelgeuse* have been obtained on Feb. 12 '93 and May 1 '96 between 5000 Å and 8000 Å with the UES (WHT, La Palma). These are available in the UES Archive (RGO Astronomy Data Centre) and have been calibrated by us. The spectra have R=49,000 with S/N∼50, for exposure times of typically 1 sec. An additional optical spectrum, also including Hα, has been obtained with the SOFIN (NOT, La Palma) on Oct. 11 '98 with medium resolution (R∼20,000). On Jul. 31 '99 a spectrum was obtained with the high-resolution camera in the near-IR (I. Ilyin, priv. comm. 1999). This wavelength range is practically free of molecular absorptions, in which we have isolated three unblended metallic absorption lines (Ni I, Cr I and Fe I) from a thorough

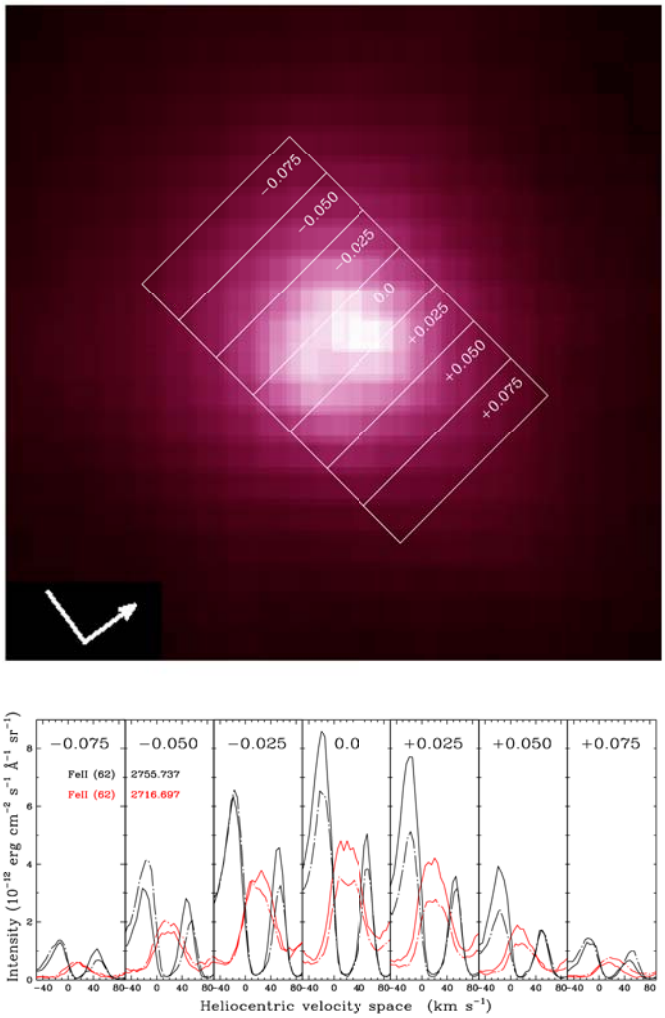

Figure 1. Combined HST Faint Object Camera exposures of α Ori of Sept. 14 '98 in the near-UV show a brightness pattern with a 'comma-like' structure. The STIS tomographic scan of about a week later shows an asymmetric distribution in the component intensity ratio of self-absorbed emission lines which results from anisotropic velocity fields in the upper chromosphere viewed across the disk. The arrow is pointing North (left is East). The aperture positions are shown in 6 off-sets of 25 mas. **Lower panel:** Solid lines are obtained in Sept. '98 and dash-dotted lines in April '98. Notice for the latter observation date the asymmetric intensity distribution with aperture position of the prominent emission line of Fe II at 2716 Å (red dash-dotted lines).

spectral synthesis analysis (R. Kurucz, priv. comm. 1999). Best LTE fits to the '98 spectrum are shown in Fig. 2 for $T_{\rm eff}$=3500 K, $\log(g)$=−0.5, microturbulence 2 km s^{-1} and $V_{\rm mac}$ & $V\sin i$ of 12 km s^{-1}. These photospheric model parameters match the strength of the TiO band-head observed near 6781 Å, also reproducing the relative intensities of the strong molecular background observed in this M-type star. Kurucz input line lists (from Schwenke 1998) contain typically a thousand TiO lines per Å. Note that this band-head is free of occasional strong atomic blends which could bias its intensity variations. We calculate that the relative intensity of this band-head saturates when reducing $T_{\rm eff}$ to 3300 K and 3200 K (black dash-dotted lines), whereas its contrast is too strong for $T_{\rm eff}$=3600 K (black dashed line). Note that the apparent weakening of this band-head with *lower* $T_{\rm eff}$ values results from the increased opacity in the overall TiO background, which decreases the contrast of the band. The spectra are scaled to its intensity maximum at 6781 Å in order to compare contrast changes over time.

3. Chromospheric model parameters

The three Hα observations are utilized to determine the chromospheric structure with non-LTE radiative transfer calculations in spherical geometry with SMULTI (Harper 1994). In Fig. 3 the spectral synthesis shows for a Kurucz photospheric model without a chromosphere, that the Hα line core submerges in the molecular and atomic background. In this case its normalized core depth does not exceed 0.2 and the line remains invisible. A chromospheric temperature and electron density structure attached to this model excites the line and matches its depth observed in '96 (with respect to the background) for a temperature minimum of 2700 K and a maximum of 5050 K, with $N_{\rm e}$=1 − 7 10^{7} cm^{-3}, extending over ≃5000 $R_{\odot}$. The normalized relative intensity of the Hα line core was deeper by 0.15 in '93, which corresponds with an increase of the chromospheric temperature by ∼400 K and slightly higher $N_{\rm e}$ values.

Our modeling requires high microturbulence values in the chromosphere in order to match the observed Hα core depth and width for a macro-broadening and $V\sin i$ of 18 km s^{-1} (and the instrumental profile). These parameters are also required to model the shape and widths of broad molecular absorption blends in the optical. Note that the Hα line core is clearly distorted and appears asymmetric due to a hyperfine splitting band of Co I lines (Kurucz 1998) in its long-wavelength wing. These highly supersonic microturbulence values mask the detection of small radial velocity variations in this line core. The wave-driven chromospheric models of Hartman & Avrett (1984) result in microturbulence values by about a factor of two smaller.

We observe a strong correlation in the depth variations of the Hα line core and the relative intensity changes of the optical TiO band-heads. Since the latter are mainly formed in the stellar photosphere, this observation strongly suggests related dynamical properties of the photospheric variability mechanism (i.e. pulsation) and the (lower) chromospheric structure. This is supported by our modeling work which shows that the weakness of the band-head at 6781 Å, observed in '96, can only be reproduced by incorporating a chromosphere in the radiative transfer calculations. Although such calculations have been per-

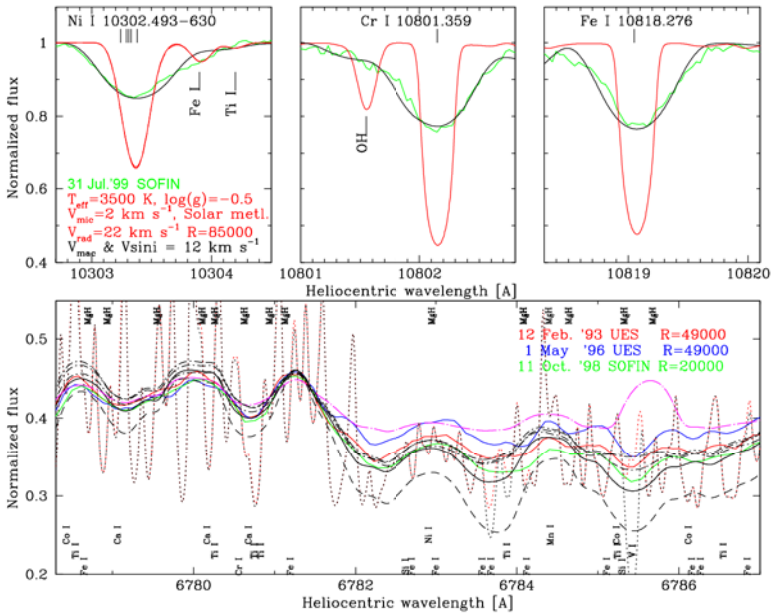

Figure 2. **Upper panels**: Photospheric model parameters are derived from best fits (black lines) to profiles of unblended metal absorption lines observed in the near-IR (green lines). **Lower panel**: The intensity of an unblended TiO band-head is best fit for $T_{\rm eff}$=3500 K (black solid line), but becomes too intense for 3600 K (black dashed line) and saturates below 3300 K (black dash-dotted lines). The weakness of the band observed in '96 (blue line) can be modeled when incorporating the chromospheric model (magenta dash-dotted line). We find that the Hα variations are correlated with the strength of these TiO bandheads. In order to compare the absorption depths the spectra have been scaled to the intensity maximum at 6781 Å. The unbroadened synthetic spectrum is shown when computed with atomic lines (black dotted line) and without (red dotted line). Note that the positions of contributing TiO and CN lines have not been labeled.

formed by us for chromospheric LTE conditions (producing un-observed strong emission lines in the optical), the weakening of this broad molecular band is in agreement with the actual band-strength observed in '96. In contrast, we found no appreciable effect on the single photospheric absorption lines from which the photospheric model parameters have been derived (Fig. 2), indicating that these lines form at photospheric depths far below the molecular bands. We therefore speculate that the different broadening velocities for the photospheric metal lines (12 $\mathrm{km\,s^{-1}}$), and for the Hα line core (and the molecular bands) formed higher (and over a larger fraction) in the photosphere (18 $\mathrm{km\,s^{-1}}$), could in part result from differences in the projected rotational or convection velocity between their mean formation heights in a very extended atmosphere.

4. Modeling chromospheric velocities

In Fig. 4 we show profile changes observed in unblended chromospheric emission lines with strongly self-absorbed cores. These resonance lines of Si I and Mg II are very sensitive to small velocity changes in the scattering circumstellar material. We detect redshifts by $\sim$8 $\mathrm{km\,s^{-1}}$ in these line cores between Jan. and Sept. '98 (the spectra are corrected for Doppler shifts due to spacecraft motion). These motions slightly increase the short-wavelength emission of the lines, indicating an average downflow in the line of sight. In the spectrum of March '99, however, the line core has displaced blueward by $\sim$4 $\mathrm{km\,s^{-1}}$, producing a strong enhancement in the red emission component, which results in a nearly symmetric line profile. The latter may indicate that the chromospheric downflow decelerated during 6 months and these velocity fields were expanding outward again thereafter. We found no correlation with the photospheric radial velocity curve simultaneously obtained in the optical at Oak Ridge Observatory. It strongly indicates a different dynamic evolution of the photospheric absorption bands and the formation height of these scattering cores in the upper chromosphere. These Doppler shifts are also apparent in the self-absorbed cores of the Mg II h & k lines, but their detailed evolution is harder to assess because these cores are strongly intensity saturated. Moreover both the short-wavelength emission components of the k and h line appear heavily mutilated by self-absorbed chromospheric resonance emission lines of Mn I.

In Fig. 5 we show best fits to the Mg II h & k lines and two Si I lines derived from our semi-empirical modeling with SMULTI. Radiative transfer in spherical geometry reproduces the relative line intensities and matches the observed line widths. We find that calculations in plane-parallel geometry with MULTI (Carlsson 1986) provide profiles which are too wide and lack sufficient core saturation. The molecular absorption background of these lines is very weak and results mainly from SiO. The strong absorption lines near 2795 Å and 2801.2 Å result from Mn I (UV 1), which become strongly self-absorbed when incorporating the chromospheric model in the radiative transfer. This core overlies the blue emission component of the k line (observed with R=114,000) and appears to contribute substantially to its permanent weakness.

We have therefore constrained the chromospheric velocity fields from detailed fits to the weaker resonance Si I lines at 2506 Å and 2516 Å. The computed atomic and molecular background (red dotted lines) shows that these are

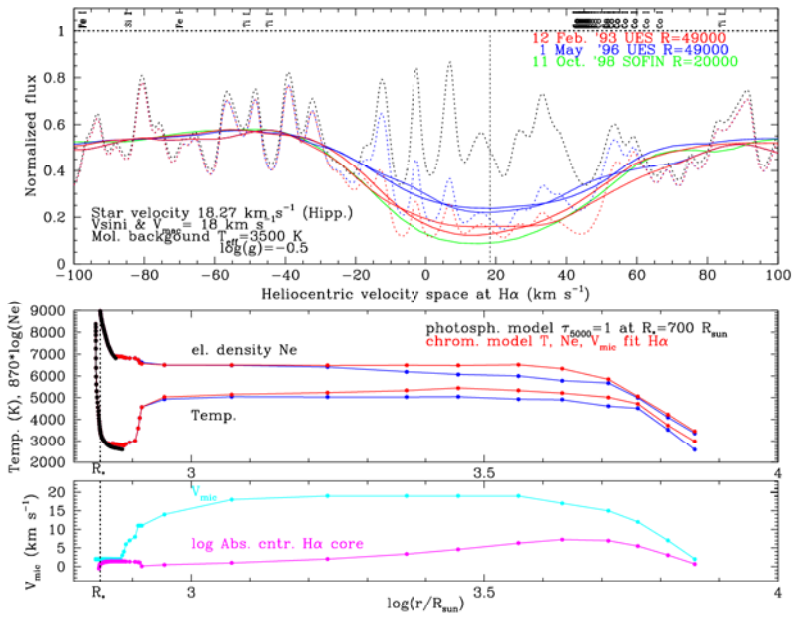

Figure 3. **Upper panel:** Three Hα profiles indicating long-term variations in the chromospheric conditions (bold lines). Our semi-empirical fits incorporate the detailed calculation of the molecular background. The Hα line core is too weak for a photospheric model without chromosphere (black dotted line). Best fits (thin solid lines) for two spectra are derived for a chromospheric model after broadening the spectrum with macroturbulence & $V\sin i$ and the instrumental profile. **Lower panels:** We find changes in the temperature structure of the outer chromosphere not exceeding ∼400 K, having supersonic microturbulence values. The absorption contribution function to the line core is also shown.

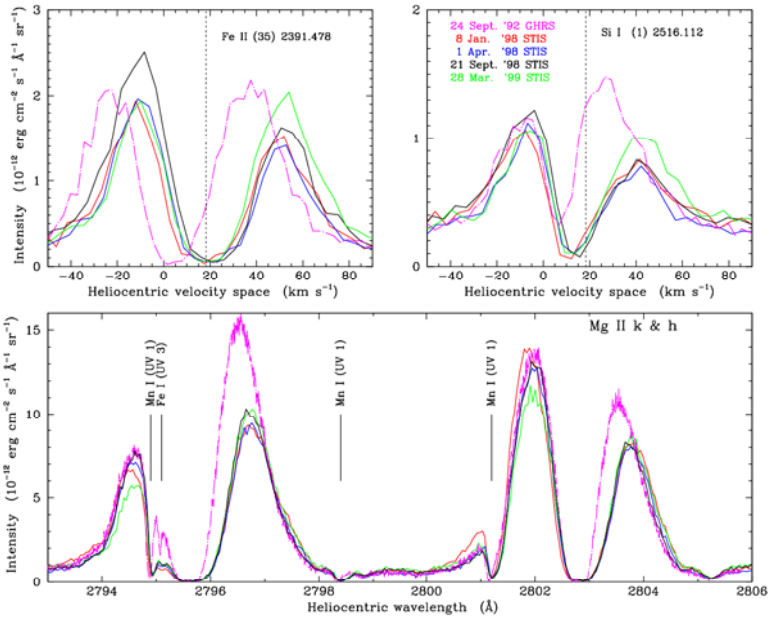

Figure 4. **Upper panels:** The evolution of self-absorbed emission line profiles at the disk center between Jan. '98 and March '99 show small Doppler shifts indicating a decelerating mean chromospheric downfall. The vertical dotted line is the HIPPARCOS star velocity of $+18.27$ km s^{-1}. A clear intensity enhancement of the long-wavelength emission is observed with a blue-shift of the core reversal (green line). **Lower panel:** This was very strong in Sept. '92, observed with HST-GHRS, indicating a phase of chromospheric expansion (magenta dash-dotted line; scaled down to the aperture size of the STIS observations). A similar blue-shift is observed in the Mn I line core which mutilates the short-wavelength Mg II k emission.

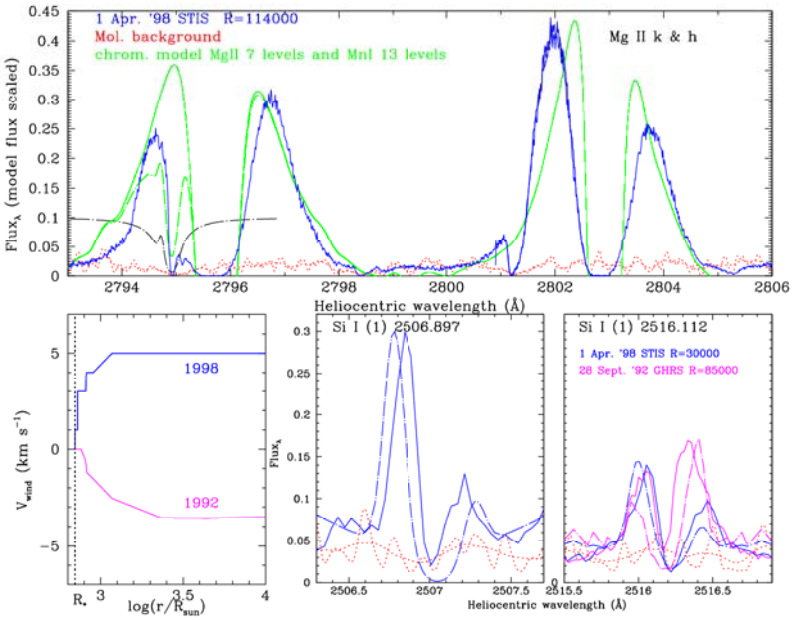

Figure 5. **Upper panel:** Detailed radiative transfer calculations (solid green lines) with the chromospheric model fit the Mg II h & k profiles observed with STIS with high dispersion (blue line). The self-absorbed core of Mn I (scaled black dash-dotted line) distorts the computed k line profile (green dash-dotted line). **Lower panels:** Best fits (dash-dotted lines) to unblended Si I lines (solid lines) constrain the velocity field in the outer chromosphere which indicates infall during '98 and outflow in '92 (panel left).

unblended lines. We apply a decelerating chromospheric downflow to model the intensity ratio of the emission wings of these lines observed in April '98. The core shifts seen in the STIS spectra during this period can be modeled with small velocity changes of 4 to 8 $\mathrm{km\,s^{-1}}$ in the outer (chromospheric) wind structure. Our radiative transfer calculations also reproduce the detailed shapes of the blue-shifted core profiles observed in GHRS spectra of Sept. '92 (Carpenter & Robinson 1997). These Doppler shifts are correlated with a strong intensity enhancement of the long-wavelength emission component. The blue-shift by about 5 to 15 $\mathrm{km\,s^{-1}}$ indicates a phase in which the outer chromosphere was strongly expanding with respect to the STIS observations of '98−'99. For this phase our chromospheric model requires an expansion velocity accelerating up to 4 $\mathrm{km\,s^{-1}}$ in order to model the observed intensity ratio of the emission components (Fig. 5). For both phases a macroturbulence & $V \sin i$ of 9 $\mathrm{km\,s^{-1}}$ is required to match the observed line widths and fluxes for both spectral resolutions.

5. Conclusions

- Spatially resolved spectroscopy of *Betelgeuse* reveals complex and varying flow patterns in the chromosphere.
- We detect chromospheric mass motions of 4 to 8 $\mathrm{km\,s^{-1}}$ between Jan. '98 and March '99. These amplitudes correspond with the amplitude of the photospheric radial velocity curve but Doppler changes appear uncorrelated.
- Intensity variations of the Hα absorption core are correlated with contrast changes of molecular band-heads, suggesting temperature effects by the chromosphere at the (photospheric) formation depths of these bands.
- Semi-empirical models of the chromosphere can be constrained by fitting Hα. These fits indicate long-term changes by $\sim$400 K in the outer chromospheric temperature structure.
- The velocity field of the outer chromosphere can be determined from detailed fits to self-absorbed emission lines observed in the near-UV. Elaborate radiative transfer calculations show that this velocity field varies over time, presently (1999) indicating a decelerating downflow.
- We detect a strong correlation between the Doppler position of these self-absorbed cores and the intensity of the longwave line emission component. This effect was particularly strong in '92 when the outer chromosphere was expanding.

Acknowledgments. This research is supported in part by STScI grant GO-5409.02-93A to the Smithsonian Astrophysical Observatory.

References

Carlsson M., 1986, Uppsala Astronomical Observatory, Report No. 33

Carpenter K. G., Robinson R. D., 1997, ApJ, 479, 970

Dupree, A. K., Lobel A., Gilliland R. L., 1999, HST Direct Ultraviolet Images of Betelgeuse, AASM 194, 66.05D

Harper G.M, 1994, MNRAS, 268, 894

Hartmann L., Avrett E. H., 1984, ApJ, 284, 238

Kurucz R. L., Proceedings of 6th Atomic Spectroscopy and Oscillator Strengths meeting in Victoria, Aug. 1998. (On Kurucz website)

Schwenke D. W., 1998, Faraday Discussion No. 109, p. 321